Ventricular Fibrillation Detection in Ventricular Fibrillation Signals Corrupted by Cardiopulmonary Resuscitation Artifact

J Ruiz, E Aramendi, S Ruiz de Gauna, A Lazkano, LA Leturiondo, JJ Gutiérrez

University of the Basque Country, Bilbao, Spain

Abstract

This study is focused on the removal of artifacts due to Cardio Pulmonary Resuscitation (CPR) on Ventricular Fibrillation ECG signals. The aim is to allow a reliable analysis of the cardiac rhythm by an AED or the defibrillation success analysis during CPR episodes. The research is based on a human model for the CPR artifact and the VF ECG signals. The test signals were generated adding the CPR artifact (noise) to the VF (signal), with a known Signal-to-Noise Ratio (SNR). The results of the adaptive Kalman filtering have been obtained according to three different levels: SNR improvement; Sensitivity improvement in the AED algorithm for the detection of shockable rhythm; and Variations of the significant frequencies, compared to the values obtained with the original VF signals. In all cases, remarkable results have been achieved regarding to the efficiency in the artifact removal.

1. Introduction

The second and third link in the adult Chain of Survival defined by the AHA (American Heart Association), are early CPR and early defibrillation, respectively [1]. However, the chest compressions and the ventilation during CPR generate a significant and typical artifact on the ECG signal, so the AED guidelines require the interruption of the CPR during the analysis. Unfortunately, several works point up the adverse effects of this suspension [2,3] and affirm the need to reduce this elapsed time to the minimum. Evidently, if the CPR artifact could be accurately removed from the ECG signal, it will clearly improve the AED efficiency.

From another approach, a significant number of studies have been focused on obtaining non-invasive methods to predict the defibrillation success. Their objective is to avoid an excessive number of shocks, which can increase the severity of the post-resuscitation myocardial dysfunction [4]. Given that the predictive information is located in the VF signal, it becomes essential to filter the interference before the ECG signal analysis.

2. Materials and methods

2.1. Background

Previous studies have been already performed using a porcine model for collecting CPR artifact and VF signal records [5-7]. It is observed that the CPR artifact spectral components are clearly distinguished from the VF signal. Therefore, the CPR artifact removal can be accomplished by linear filtering.

More advanced studies [8-10] have introduced a human model for the VF signals, maintaining a porcine model for the CPR artifacts. In this case, there is a remarkable overlapping between both the artifact and the ECG signal spectral distribution. For this reason, LMS (Least-Mean-Square) adaptive filtering techniques have been applied with good results in artifact removal. But, two main limitations are attributed to the described methods. A piston device is used to induce the CPR artifacts, giving a constant fundamental frequency and also a constant compression depth. Besides, these techniques require reference signals such as the compression depth and the transthoracic impedance, strongly correlated to the CPR artifact, and not easily available in a real-life situation.

Our contribution is to face the CPR artifact removal applying a human model for both the CPR artifact and the VF signal. Also, the applied technique, based on an adaptive Kalman filter, avoids the need for reference signals.

2.2. Working database

Unfortunately, the Emergency Services sometimes arrive when the patient presents already an asystolic rhythm. If the AED first analysis results in a non-shockable rhythm diagnosis, it is required to start the CPR. At this time, the signal that is being recorded is directly the CPR artifact. Thus, two Electrophysiology specialists from the Basurto Hospital of Bilbao (Spain), certified 17 CPR records, which were processed with a sampling frequency of 250Hz.

200 coarse VF records were obtained from the human VF rhythms database that was developed by Osatu S. Coop. for testing the AED algorithm for the

detection of shockable rhythms. Employing decimation and interpolation techniques, all the VF records were processed with the sampling frequency of 250Hz.

Finally, each record has been filtered (using a band pass filter 0.5-30Hz) to suppress DC, baseline drifts and possible electrical network interference.

2.3. Preliminary spectral analysis

The spectral characteristics of the 17 CPR artifacts have been analyzed using a Welch estimator with a Hanning window of 4.8 seconds. From the study of the SPD (Spectral Power Density) of each record, it can be confirmed that due to the periodic pattern of the CPR artifact, the power is distributed around the fundamental frequency and its harmonics. The same spectral analysis has been developed for the 200 VF records.

Fig. 1 shows the averaged SPD for all the CPR artifact and all the VF windows, showing a clear overlapping. Moreover, taking into account the strong SPD variability of the signals under study, an adaptive filtering technique is proposed to distinguish and remove the CPR artifact from the VF ECG signal.

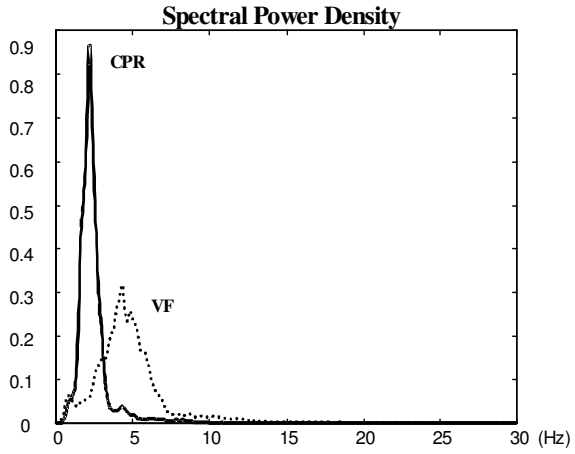

Figure 1. Averaged SPDs for all the CPR artifact and VF signal windows

2.4. Test signals

The signals for testing the proposed filter have been generated by adding the CPR artifact to the pure VF signal with a fixed noise level. SNR (Signal to Noise Ratio) of –10, -6, -3 and 0dB have been considered to obtain the set of test signals.

2.5. Description of the designed Kalman filtering technique

The CPR artifact removal from the VF signal by means of adaptive Kalman filtering assumes that the studied system can be described by two state space matrix equations:

- The state transition equation:

$$\underline{s}(n+1) = \underline{A}(n+1)\,\underline{s}(n) + \underline{w}(n+1) \quad (1)$$

- The observation equation:

$$\underline{z}(n) = \underline{H}(n)\,\underline{s}(n) + \underline{u}(n) \quad (2)$$

The *M*-vector $\underline{s}(n)$ contains the values of the *M* parameters that define the state of the system at the time *n* and is, thus, the state vector. The *(M x M)* matrix $\underline{A}(n)$ is the state transition matrix and the *(L x M)* matrix $\underline{H}(n)$ is the observation matrix. The *M*-vector $\underline{w}$ and the *L*-vector $\underline{u}$ are uncorrelated, zero mean and white, with covariances $\underline{W}$ and $\underline{U}$, respectively.

Optimal estimates of the state vector $\underline{s}(n)$ are generated recursively from the sequence of noisy observations $\underline{z}(n)$ using the following equations. The notation $\hat{\underline{s}}(n/j)$ reads "the estimate of $\underline{s}(n)$ given data from sample 0 to sample *j*".

- The estimation equation:

$$\hat{\underline{s}}(n/n) = \hat{\underline{s}}(n/n-1) + \underline{K}(n)\left[\underline{z}(n) - \underline{H}(n)\,\hat{\underline{s}}(n/n-1)\right] \quad (3)$$

- The prediction equation:

$$\hat{\underline{s}}(n/n-1) = \underline{A}(n)\,\hat{\underline{s}}(n-1/n-1) \quad (4)$$

- The Kalman gain equation:

$$\underline{K}(n) = \underline{V}(n/n-1)\,\underline{H}^T(n)\left[\underline{H}(n)\,\underline{V}(n/n-1)\,\underline{H}^T(n) + \underline{U}(n)\right]^{-1} \quad (5)$$

- The error covariance equations:

$$\underline{V}(n/n-1) = \underline{A}(n)\,\underline{V}(n-1/n-1)\,\underline{A}^T(n) + \underline{W}(n) \quad (6)$$

$$\underline{V}(n-1/n-1) = \underline{V}(n-1/n-2) - \underline{K}(n-1)\,\underline{H}(n-1)\,\underline{V}(n-1/n-2) \quad (7)$$

Where:

$$\underline{V}(n/n) = E\left\{(\underline{s}(n) - \hat{\underline{s}}(n/n))\,(\underline{s}(n) - \hat{\underline{s}}(n/n))^T\right\} \quad (8)$$

$$\underline{V}(n/n-1) = E\left\{(\underline{s}(n) - \hat{\underline{s}}(n/n-1))\,(\underline{s}(n) - \hat{\underline{s}}(n/n-1))^T\right\} \quad (9)$$

The system matrices $\underline{A}$, $\underline{W}$, $\underline{H}$, and $\underline{U}$ may be time varying, but they are assumed to be known a priori.

In our case, the observed signal is identified as the noisy observation vector $\underline{z}(n)$ and, as at each time *n* there is a unique observation, then *L=1*. The system state transition and observation equations have been described, assuming that the CPR artifact as well as the VF signal can be modeled by a sinusoidal function of a known angular frequency ω_a and ω_s, respectively.

The system state variables are identified as:

$$\underline{s} = \begin{Bmatrix} A_a\cos\varphi_a \\ A_a sen\varphi_a \\ A_s\cos\varphi_s \\ A_s sen\varphi_s \end{Bmatrix} \quad (10)$$

where A_a, A_s, φ_a and φ_s are the CPR artifact and the VF signal amplitudes and phases, respectively. They are assumed constant so that the state transition matrix is identified with the (4x4) identity matrix. From this approach, the observation matrix is identified at each time with:

$$\underline{H}(n) = \left[\cos\omega_a n \quad -sen\,\omega_a n \quad \cos\omega_s n \quad -sen\,\omega_s n\right] \quad (14)$$

The covariance diagonal (4x4) matrix $\underline{W}$ and (1x1) matrix $\underline{U}$ are assumed to be constant all through the iterative process and their values have been

experimentally fixed. It has been checked that, in a wide range, they present a very little influence on the filtering iterative process.

The application of the iterative process to the proposed modeling requires knowing ω_a and ω_s. Both angular frequencies are assumed constant all through the time window of 4.8s and are estimated from the considered window SPD. The ω_a value is the angular frequency in which the SPD presents a maximum in the 0-2.8 Hz interval; ω_s is calculated as the angular frequency in which the SPD presents a maximum amplitude peak in the 3.2-7.5 Hz interval.

3. Results

For the global evaluation of the proposed filtering technique, we have thoroughly analyzed the Kalman filter efficiency in recovering three significant parameters of the VF ECG signal.

3.1. SNR improvement

The 17 CPR records have been tested combined with all the 200 VF records, for the original SNR values of -10, -6, -3 and 0dB.

Fig. 2 shows the SNR values obtained after applying the Kalman filter to each test signal. They are compared in the figure with each original value. It is observed that the SNR improvement is quite significant and depends strongly on the added CPR artifact.

3.2. Sensitivity improvement

The sensitivity improvement in the AED algorithm for the detection of shockable rhythms has been analyzed. For the same original SNR values, the AED sensitivity has been characterized after filtering.

Table 1 presents the sensitivity evaluated with and without the Kalman filtering, again for each CPR artifact and for each original SNR. It is observed a high improvement applying the Kalman filtering technique. For all the CPR artifacts the sensitivity after filtering gets close to the original value of nearly 100%.

3.3. Significant frequencies variations

We have analyzed three significant frequencies for both the original 200 VF records and the recovered VF ones:

1. The median frequency, f_m: frequency below which the spectrum power is the 50%.
2. The dominant frequency, f_d: that corresponding to the maximum power spectrum.
3. The edge frequency (f_e): frequency below which the spectrum power is the 95%.

These values have been re-calculated after filtering for the same original SNR values. It can be observed in Table 2 that with all the combinations, the average values obtained are in the range of those calculated for the original ones.

4. Conclusions

In this paper, we have described an adaptive Kalman filtering technique to suppress the CPR artifact from the VF signal in a human model.

Our model is very simple, as it only needs four state variables to be defined. However, additional signal spectral information is needed to know it properly.

The efficiency of this technique has been tested calculating SNR improvement, AED sensitivity improvement and variations of the VF signal characteristic frequencies.

The achieved results are promising, so we think that some future works should be focused on increasing the number of test CPR artifact records and also on optimizing the adaptive filter model.

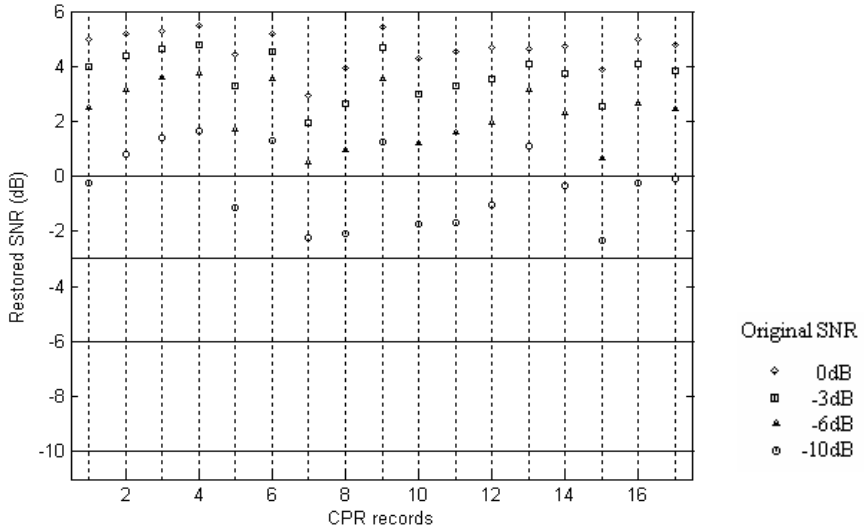

Figure 2. SNR improvement evaluation

Table 1. Sensitivity evaluation in %

	SNR= -10dB		SNR= -6dB		SNR= -3dB		SNR= 0dB	
	No filter	Filter	No filter	Filter	No filter	Filter	No filter	Filter
CPR1	70.6806	98.4293	46.0733	100	31.9372	98.9529	37.6963	98.9529
CPR2	49.7382	94.2408	40.3141	98.4293	34.555	98.9529	33.5079	98.9529
CPR3	16.2304	92.1466	34.555	97.3822	36.1257	96.8586	52.8796	98.9529
CPR4	4.712	94.7644	16.7539	98.4293	39.267	99.4764	55.4974	99.4764
CPR5	8.377	96.8586	37.6963	97.3822	45.0262	99.4764	62.8272	97.3822
CPR6	7.8534	96.3351	24.0838	99.4764	42.4084	99.4764	60.2094	97.9058
CPR7	7.8534	99.4764	27.2251	97.9058	46.0733	97.3822	71.2042	97.3822
CPR8	80.6283	84.8168	85.8639	95.8115	81.1518	96.3351	69.1099	97.9058
CPR9	34.555	95.288	47.1204	99.4764	62.8272	98.9529	76.4398	98.9529

	SNR= -10dB		SNR= -6dB		SNR= -3dB		SNR= 0dB	
	No filter	Filter	No filter	Filter	No filter	Filter	No filter	Filter
CPR10	38.2199	91.623	74.8691	94.7644	81.1518	97.3822	74.8691	96.8586
CPR11	18.8482	100	43.4555	100	53.4031	100	65.445	100
CPR12	12.0419	100	27.2251	98.9529	35.0785	98.9529	49.2147	98.4293
CPR13	0	97.9058	5.7592	99.4764	23.0366	99.4764	35.6021	98.9529
CPR14	65.445	98.4293	68.0628	98.4293	70.1571	99.4764	69.1099	100
CPR15	79.0576	97.3822	86.911	98.4293	80.1047	99.4764	64.3979	100
CPR16	46.0733	94.7644	51.3089	98.4293	71.2042	100	83.7696	100
CPR17	59.6859	91.0995	69.1099	93.7173	56.0209	97.3822	52.8796	97.9058

Table 2. Mean frequency values restored after filtering the VF+CPR signal with different SNR

	f_m : 4.4470 ± 1.1003 Hz				f_d : 4.4152 ± 1.2364 Hz				f_e : 8.9229 ± 2.9374 Hz			
	-10dB	*-6dB*	*-3dB*	*0dB*	*-10dB*	*-6dB*	*-3dB*	*0dB*	*-10dB*	*-6dB*	*-3dB*	*0dB*
CPR1	4.354	4.4468	4.5079	4.5549	4.4304	4.4603	4.5236	4.5316	6.1796	6.1342	6.1169	6.1274
CPR2	4.3484	4.4703	4.5664	4.6205	4.438	4.4864	4.5708	4.6182	6.1256	6.0946	6.1159	6.1319
CPR3	4.3093	4.5205	4.5805	4.623	4.4958	4.5947	4.6094	4.6132	5.8884	6.017	6.0698	6.1
CPR4	4.4015	4.543	4.5896	4.6235	4.5205	4.5831	4.6066	4.6179	6.3174	6.2852	6.2149	6.1877
CPR5	4.4173	4.5191	4.5752	4.6231	4.4745	4.561	4.5743	4.631	6.1964	6.1459	6.1391	6.157
CPR6	4.3666	4.4801	4.5155	4.5633	4.4127	4.4921	4.5063	4.5315	6.1667	6.1321	6.0989	6.1155
CPR7	4.5962	4.6372	4.6474	4.6417	4.5066	4.5219	4.5461	4.5572	7.2737	6.9583	6.6741	6.3736
CPR8	4.2651	4.4839	4.5711	4.6111	4.1846	4.5185	4.5473	4.5906	7.3842	7.0445	6.7137	6.4793
CPR9	4.2481	4.4431	4.4917	4.53	4.3298	4.4858	4.5122	4.529	6.1484	6.1374	6.1133	6.1289
CPR10	4.7437	4.6962	4.6928	4.6744	4.6674	4.6457	4.6659	4.661	8.5221	8.0396	7.4926	6.9807
CPR11	4.0724	4.317	4.4314	4.5024	4.1085	4.3633	4.4407	4.4986	5.2425	5.4914	5.6765	5.8308
CPR12	4.5653	4.6273	4.6233	4.6171	4.6065	4.6252	4.6287	4.5992	6.53	6.4076	6.3541	6.2709
CPR13	4.2695	4.4754	4.5804	4.6077	4.2215	4.4413	4.5623	4.5769	6.016	6.0517	6.1214	6.1068
CPR14	4.4282	4.5426	4.5874	4.6346	4.5327	4.609	4.6162	4.6388	6.8042	6.5406	6.3817	6.3018
CPR15	4.4927	4.5366	4.5692	4.6219	4.547	4.5506	4.572	4.6117	6.5884	6.2562	6.2122	6.2003
CPR16	4.1676	4.4443	4.5514	4.6098	4.2201	4.462	4.5457	4.5987	6.3137	6.2644	6.2247	6.2276
CPR17	4.596	4.6353	4.6735	4.6967	4.6923	4.6848	4.7051	4.7198	6.5766	6.3871	6.3224	6.2365

Acknowledgements

The authors would like to thank Osatu S. Coop. and the Basurto Hospital in Bilbao (Spain) for their contribution to this work.

References

[1] AHA and the Internal Liaison Committee on Resuscitation. Guidelines 2000 for Cardiopulmonary Resuscitation and Emergency Cardiovascular Care: International Consensus on Science. Circulation 2000.

[2] Cobb LA, Fahrenbruch CE, Walsh TR, Copass MK, Olsufka M, Breskin M et al. Influence of CPR prior to defibrillation in patients with out-of-hospital ventricular fibrillation. The Journal of the American Medical Association 1999;281,13:1182-8.

[3] Sato Y, Weil MH, Sun S, Tang W, Xie J, Noc M et al. Adverse effects of interrupting precordial compression during cardiopulmonary resuscitation. Critical Care Medicine 1997;25:733-6.

[4] Xie J, Weil MH, Sun S, Tang W, Sato Y, Jin X et al. High-energy defibrillation increases the severity of postresuscitation myocardial dysfunction. Circulation 1997;96:683-8.

[5] Strohmenger HU, Lindner KH, Keller A, Lindner IM, Pfenninger EG. Spectral analysis of ventricular fibrillation and closed-chest cardiopulmonary resuscitation. Resuscitation 1996;33:155-61.

[6] Noc M, Weil MH, Tang W, Sun S, Pernat A, Bisera J. Electrocardiographic prediction of the success of cardiac resuscitation. Critical Care Medicine 1999;27,4:708-14.

[7] Hamprecht FA, Achleitner U, Krismer AC, Lindner KH, Wenzel V, Strohmenger HU et al. Fibrillation power, an alternative method of ECG spectral analysis for prediction of countershock success in a porcine model of ventricular fibrillation. Resuscitation 2001;50:287-96.

[8] Langhelle A, Eftestøl T, Myklebust H, Eriksen M, Holten BT, Steen PA. Reducing CPR artifacts in ventricular fibrillation in vitro. Resuscitation 2001;48:279-91.

[9] Aase SO, Eftestøl T, Husøy JH, Sunde K, Steen PA. CPR artifact removal from human ECG using optimal multichannel filtering. IEEE Transactions on Biomedical Engineering 2000;47,11:1440-9.

[10] Eilevstjønn J, Husøy JH, Eftestøl T, Aase SO, Steen PA. Multichannel adaptive filtering using an efficient matching pursuit-like algorithm for removal of CPR artifacts in ECG signals. IEEE Transactions on Biomedical Engineering 2002;4:3864-7.

Address for correspondence.
Jesús Ruiz
Department of Electronics and Telecommunications
Engineering School of Bilbao
Alameda Urquijo, s/n
48013-BILBAO (Spain)
E-mail address: jtpruojj@bi.ehu.es